Gamma-ray Measurements with LaBr3: Ce Detectors – thinking Outside the Box

Available online at www.sciencedirect.com

SciVerse ScienceDirect

Physics Procedia 31 (2012) 21 – 28

Physics Procedia

Gamma-ray measurements with $LaBr_3 : Ce$ detectors - thinking outside the box

A. Oberstedt[a,b,*], R. Billnert[b,c], S. Oberstedt[c]

[a] *Akademi för Naturvetenskap och Teknik, Örebro Universitet, S-70182 Örebro, Sweden*
[b] *Fundamental Fysik, Chalmers Tekniska Högskola, S-41296 Göteborg, Sweden*
[c] *European Commission, DG Joint Research Centre (IRMM), B-2440 Geel, Belgium*

Abstract

Recently developed cerium-doped lanthanum bromide ($LaBr_3 : Ce$) scintillation detectors have shown to possess promising properties with respect to the detection of γ-rays compared to previously known materials. In this work however, we demonstrate how these detectors may be used to obtain information not only about γ-rays, but also about neutrons, i.e. thinking "inside" and "outside" the box, respectively. For this purpose γ-rays were detected in coincidence with fission fragments and both their energy and their time-of-flight relative to the instant of a fission event is recorded. By evaluating the time-of-flight distributions of γ-rays, identified as decays of excited states after population by inelastically scattered neutrons inside the scintillation crystal as well as other surrounding materials, we show that it is possible to acquire knowledge from and about the spectrum of incident neutrons. We give three examples for conceivable applications, used to determine geometrical profiles, cross sections and neutron spectra, respectively.

Keywords: Neutron measurements, Lanthanum bromide, Time-of-flight, ^{252}Cf(sf), ^{79,81}Br(n,n'), ^{235}U(n$_{th}$,f)
07.85.Nc, 29.30.Kv, 29.40.Mc

1. Introduction

In recent years new scintillators materials like cerium-doped lanthanum chloride and bromide as well as cerium bromide have been developed and proven to have promising features for the detection of γ-rays compared to previously known materials. We too have conducted extensive investigations of these novel detectors and determined their characteristic properties [1, 2]. We found that these detectors in fact constitute an appropriate choice for the assessment of prompt fission γ-ray energy spectra and multiplicities, as requested by the Nuclear Energy Agency [3]. Especially the good timing resolution (better than 350 ps) allows clean separation of γ-rays depending on the different processes of their creation by means of the time-of-flight method. First experiments have been performed with $LaCl_3 : Ce$ detectors and results from the reactions ^{235}U(n$_{th}$,f) and ^{252}Cf(sf) have already been published [2, 4, 5]. Recently, we reported on the measurement of γ-rays from the reaction ^{252}Cf(sf) with a $LaBr_3 : Ce$ detector [6]. In this experiment we used an ultra-fast poly-crystalline chemical vapor deposited (pcCVD) diamond detector as fission trigger that provided the start signal for the coincident measurement of γ-rays. Due to the different time-of-flight between photons and neutrons, prompt fission γ-rays were easy to distinguish from γ-rays induced by reactions involving fast and slow

*Corresponding author
Email address: andreas.oberstedt@oru.se (A. Oberstedt)

doi:10.1016/j.phpro.2012.04.004

neutrons, i.e. basically by (n,n') and (n,p) or (n,γ) reactions, respectively. During the analysis of (n,n') data, the idea emerged to use this reaction to monitor neutron fields. In this work, we report on the measurement of γ-rays emitted in coincidence with the spontaneous fission of ^{252}Cf with a 2 in. $\times$ 2 in. $LaBr_3 : Ce$ scintillation detector.

After a brief description of the experimental set-up, we show how well γ-rays produced in different reactions may be distinguished by their characteristic time-of-flight. Then we focus on the analysis of γ-rays from neutrons inelastically scattered inside the scintillation crystal and other surrounding material and give examples for how this data may be used to obtain information about

- the geometrical profile of an extended scattering object
- the cross section of the neutron-induced reaction as function of energy
- the energy spectrum of neutrons from the reaction ^{235}U(n$_{th}$, f)

We present and discuss recent results, before finishing up with conclusions and giving an outlook over upcoming efforts and improvements.

2. Some experimental details

The $LaBr_3 : Ce$ crystal of size 2 in. $\times$ 2 in. (51 mm in diameter and 51 mm in thickness) in the coaxial BrilLanCe^{TM}380 detector used in this work was manufactured by Saint-Gobain Crystals [7] and attached to a Hamamatsu R6231-100 photomultiplier tube (PMT). The properties of the detector have been determined and the results are described in more detail elsewhere [8]. However, at least some important properties should be mentioned here as well. The resolving power was determined to 2.5% at 662 keV (^{137}Cs), following very well the expected $E^{-1/2}$ behavior. The full peak efficiency for γ-rays of same energy was found to be 34%, and an intrinsic timing resolution of (338 $\pm$ 18) ps (FWHM) was determined for ^{60}Co γ-rays by putting a threshold on the pulse height just below the full energy peaks, corresponding to about 1000 keV. In general, we observed that our data were in good agreement with the specifications given by the manufacturer [9].

Fission - photon coincidences were then measured with a ^{252}Cf source, placed in the (2v, 2E) fission fragment spectrometer VERDI (VElocity foR Direct particle Identification), a two-arm time-of-flight chamber, which allows measuring pre- and post-neutron masses directly and simultaneously, avoiding prompt neutron corrections [10]. In this work, however, VERDI was operated in single-arm mode. In this constellation a polycrystalline diamond detector of size 2.5 mm $\times$ 10 mm and thickness 100 μm was placed on top of the ^{252}Cf source, on the opposite side of the flight path, providing an intrinsic timing resolution better than 150 ps for fission-fragments [11]. At a distance of 30 cm from the source, the 2 in. $\times$ 2 in. $LaBr_3 : Ce$ detector was positioned for measuring γ-rays. The signals from the anode output were split and the two branches were used for the determination of timing and pulse height, respectively, then digitized and collected in list-mode for further treatment with the software package GENDARC [12]. The ^{252}Cf sample has a radius of 2.5 mm with an original α-activity of 10 μCi at the date of its production (October 31, 2007) [13]. At the time of the experiment described in this work, the sample provided 1.101×10^4 fission fragments/s in 4π. The geometrical efficiency of the diamond detector for fission fragments was 46.18%.

3. Results

The result of the simultaneous measurement of time-of-flight versus γ-energy is shown in Fig. 1, properly calibrated in time and energy. In this two-dimensional presentation of the detected γ-rays, different time-of-flight (TOF) regions may be distinguished. The region of prompt fission γ-rays is indicated by the dashed line. Below this line, many (vertical) γ-lines are observed, whose time distributions all have in common that they start right after the detection of prompt fission γ-rays. We conclude that their origin is attributed to inelastic neutron scattering in the detector or in structural materials in the vicinity of the experimental set-up. Moreover, depending on neutron energy, the time distribution for a given de-excitation ends, where the corresponding time-of-flight of a neutron is in accordance with its kinetic energy. This is indicated by the dotted line, which connects the time-of-flight of neutrons with a certain energy, traveling the distance between ^{252}Cf sample and $LaBr_3 : Ce$ detector. Events at higher values for the time-of-flight are considered as background due to random coincidences, caused by either intrinsic radioactivity or excitations

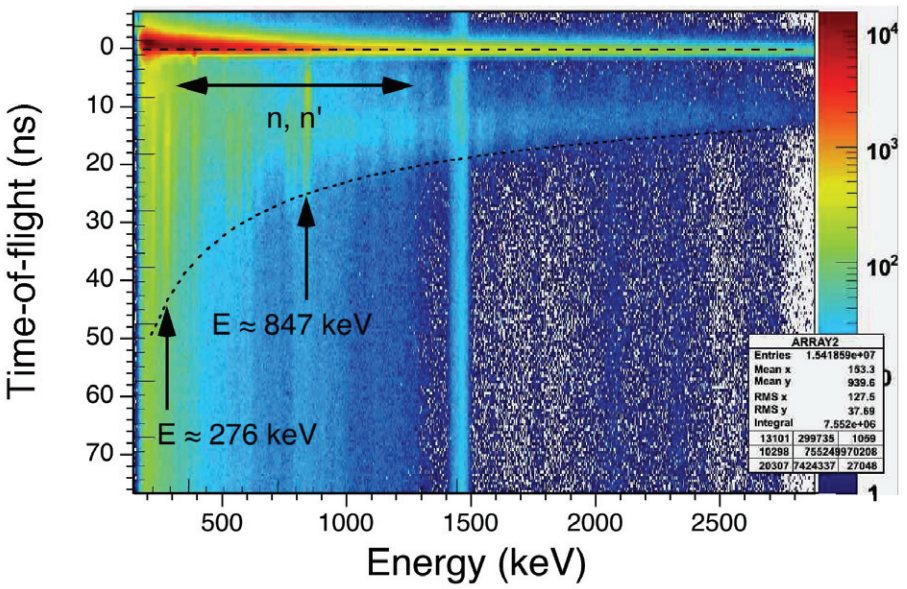

Figure 1: Distribution of γ-rays by time-of-flight vs. pulse height. Prompt fission γ-rays are represented by a horizontal area (dashed line), while the vertical lines represent γ-rays from reactions induced by prompt fission neutrons, preferably inelastic scattering (see text for details).

by scattered and thermalized neutrons as well as Compton-scattered γ-rays, since entirely uncorrelated with the instant of a fission event.

In this chapter we take a closer look at the time-of-flight distributions of γ-rays with energies 276 and 847 keV, which are both indicated in Fig. 1. The first γ-line is identified as the decay of the first excited state in ^{81}Br, which is present in the crystal of the $LaBr_3 : Ce$ detector. The γ-rays with E = 847 keV are assigned to the decay of the first excited state in ^{56}Fe, of which a considerable amount is found in the structural material of VERDI. The following sections are dedicated to the results that were derived from the analysis of those γ-rays and results from a similar experiment, where the neutron source was fission neutrons from the reaction ^{235}U(n$_{th}$,f) instead of ^{252}Cf(sf).

3.1. Geometrical profile of an extended object

Putting a window around the events with E_γ = 847 keV, which are indicated in Fig. 1, allows investigating the corresponding time-of-flight distribution. This distribution is shown in Fig. 2, where dashed lines are used to separate the characteristic time regimes for prompt fission γ-rays, photons from the decay of isomers and inelastic neutron scattering, as well as for other background photons, whose origin is described above. The full drawn line indicates the distribution of all background contributions, whose subtraction leaves the time spectrum solely due to the decay of excited ^{56}Fe created by inelastically scattered neutrons. The resulting time distribution should be able to be explained by means of the incident neutron spectrum and the excitation function of the involved reaction. Both are known; the first is described as Maxwell-Boltzmann distribution [14, 15], the second was taken from the evaluated data library ENDF/B-6.8 [16]. With this information at hand neutron time-of-flight spectra were calculated for different path lengths from 10 to 40 cm in steps of 5 cm and fitted to the experimental data. The result is depicted in Fig. 3, showing an excellent agreement between the simulated distribution (thick red curve) and the experimental spectrum (black curve). The relative contributions from ^{56}Fe plotted as a function of distance between neutron source and iron material give a nice reproduction of the one-dimensional geometrical profile of the fission fragment spectrometer VERDI (cf. Fig. 4).

3.2. Inelastic neutron scattering cross-section measurements on ^{79,81}Br

Following the procedure described in the previous section, we put then our focus on the investigation of the 276 keV γ-rays, also indicated in Fig. 1. After assessing and subtracting all other components in the corresponding time-of-flight spectrum than the one due to inelastically scattered neutrons, we aimed at determining the cross sections

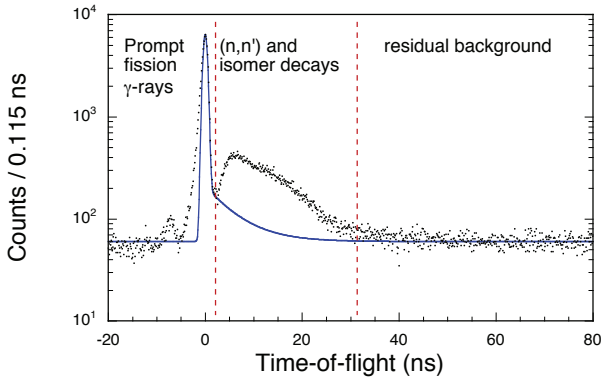

Figure 2: Time-of-flight distribution of γ-rays with E = 847 keV. Three different regions are indicated by dashed lines and the measured time spectrum is compared to the assessed background, shown as full drawn line.

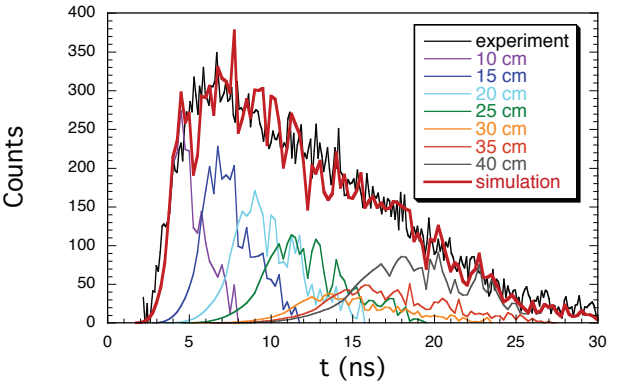

Figure 3: Background subtracted time-of-flight spectrum of γ-rays with E = 847 keV (in black) together with the result of simulated distributions for fission neutrons traveling between the ^{252}Cf source and a ^{56}Fe scatterer, fitted to the experimental data.

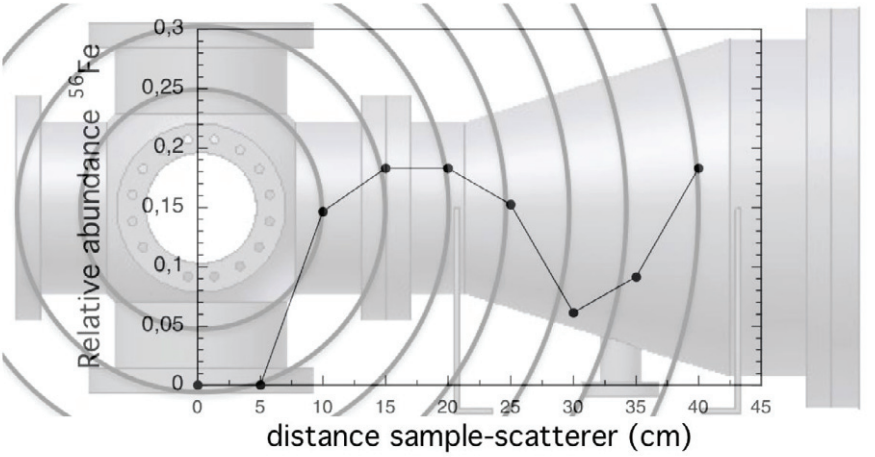

Figure 4: Experimentally obtained ^{56}Fe distribution, i.e. the presence of ^{56}Fe as function of distance from the neutron source. A drawing of the fission fragment spectrometer VERDI is shown as background to explain the observed spatial distribution.

for the involved reactions. In order to do so, we took a closer look at the γ-rays inside the chosen energy window. What appeared to be one peak at 276 keV (cf. Fig. 1), turned out to consist of two peaks, which are identified as the result of de-excitations of the third excited state in ^{79}Br at 261.31 keV and the first excited state in ^{81}Br at 275.986 keV (cf. Fig. 5), populated in the reactions ^{79}Br(n,n'3) and ^{81}Br(n,n'1), respectively. Both isotopes are present in ^{nat}Br and, therefore, in the detector crystal as well, which is the scattering material here. Hence, a new time-of-flight distribution was generated for a γ-energy region from 279 to 297 keV, containing 40% of the total intensity of the peak at 276 keV. Re-normalizing this time-of-flight distribution to 100% and subtracting it from the one for the entire energy interval, i.e. from 244 to 297 keV, results in a corresponding time-of-flight distribution for the 261 keV peak. From the detected rate of γ-rays as a function of energy, $R_{det}(E)$, and according to the relation

$$R_{det}(E) = \overline{\epsilon_\gamma} \cdot R(E), \tag{1}$$

with $\overline{\epsilon_\gamma} = 0.45$ (efficiency for 276 keV γ-rays averaged over the entire detector volume, simulated from $\epsilon_\gamma = 0.74$ determined for external irradiation), and where the reaction rate is given by

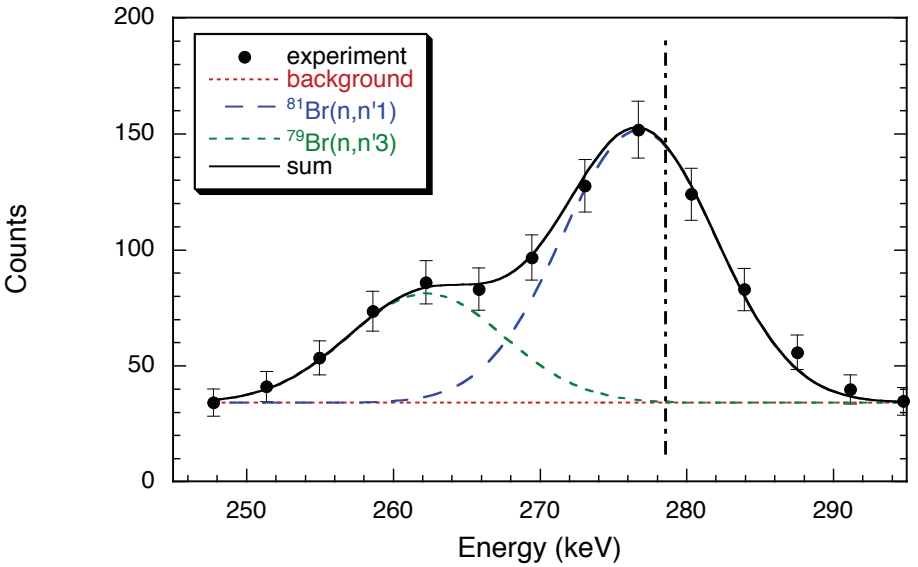

Figure 5: Part of the energy spectrum of γ-rays showing the window, for which the time distribution was examined. The peak area to the right of the vertical dashed-dotted line corresponds to 40% of the total intensity of the 276 keV transition.

$$R(E) = N \cdot I(E) \cdot \sigma(E), \tag{2}$$

with N = number of relevant nuclei in the detector volume (known) and $I(E)$ = neutron current (known from the activity of the ^{252}Cf source), the excitation function $\sigma(E)$ may be determined for both reactions ^{79}Br(n,n'3) and ^{81}Br(n,n'1). The results are shown in Fig. 6, where the experimental values are compared to data published in the evaluated libraries JENDL-4.0, ENDF/B-VII.0 and JEFF-3.1.1, provided by the data bank of the Nuclear Energy Agency [17]. Although these data libraries contain quite diverging values, the general trend is reproduced by the experimental data. However, so far it seems not possible to judge, which library data is to favor by our results. Still, it should be mentioned that the relative intensities of both excitations found in this work are best described by the data from JENDL-4.0.

3.3. $^{235}U(n_{th}, f)$ fission neutron measurements

This section is dedicated to a first demonstration of measuring a neutron spectrum by analyzing γ-rays produced by inelastic neutron scattering off bromine nuclei in a $LaBr_3 : Ce$ detector. However, prior to this the neutron detection efficiency had to be determined. According to Eqs. 1 and 2, the intrinsic neutron efficiency may be expressed as

$$\epsilon_n = R_{det}(E)/R_{hit}(E), \tag{3}$$

where the neutron detection rate $R_{det}(E)$ is known from the measured time-of-flight distribution and the hit rate $R_{hit}(E)$ may be calculated from the activity of the neutron source, the geometry between source and detector, and the shape of the neutron spectrum of ^{252}Cf. The result is shown in Fig. 7 together with the result of a fit and its uncertainty.

After having derived the energy dependent neutron efficiency, we applied it to data taken in a preceding experiment, where the major aim was to measure prompt fission γ-rays from the reaction ^{235}U(n_{th},f) in coincidence with fission fragments. It was performed at the 10 MW research reactor of the Institute of Isotopes HAS in Budapest, Hungary, also employing the fission fragment spectrometer VERDI, which that time contained a ^{235}U sample of mass 113 μg. While more information about this experiment may be found in Refs. [4, 5], we focus here on γ-rays after inelastic neutron scattering, measured with the $LaBr_3 : Ce$ detector described above. However, during this measurements we encountered some problems with this detector, or rather with the dynode output of the photomultiplier tube (PMT) that was used for the energy signal. The simultaneous use of the anode and dynode output of the PMT caused

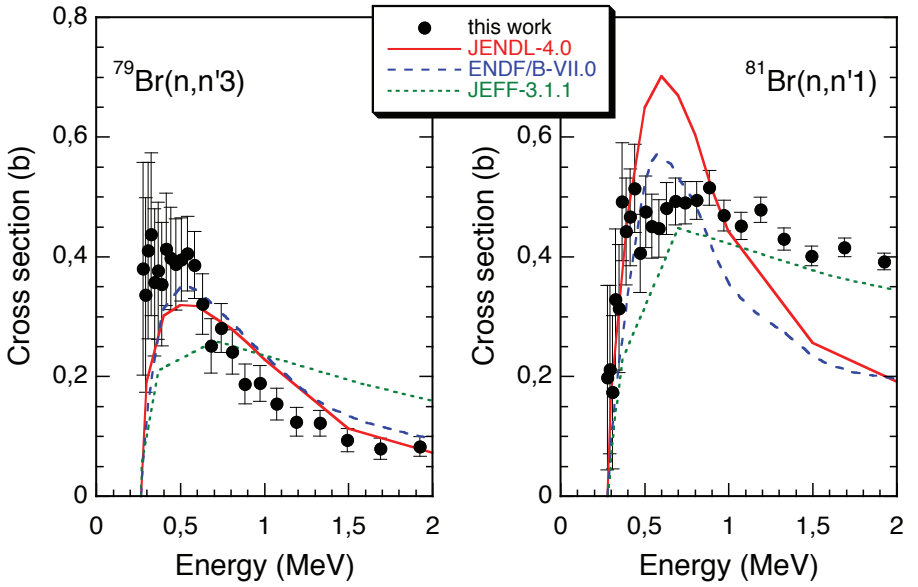

Figure 6: Excitation functions for the reactions ^{79}Br(n,n'3) and ^{81}Br(n,n'1). Experimental results are compared to data from different evaluated libraries.

a pulse height dependent shift of the timing signal. Still, we decided to analyze the data further. More details and a description of which corrections we had to apply will be given elsewhere [8].

In a presentation similar to the one in Fig. 1, an energy window of same size as above on 276 keV γ-rays was selected and for those events a time-of-flight distribution was generated. Eventually, a neutron spectrum, corrected with the efficiency according to Fig. 7 is obtained and shown in Fig. 8. Due to the just mentioned complications during the measurement, we had to make certain restrictions. Since we could not be sure that the correction procedure for prompt fission γ-rays may be applied to other TAC regimes, we considered only events close to these events, i.e. those with a short time-of-flight and thus corresponding to higher neutron energies. Because of the difficulties of properly assessing the background due to isomer decays, we also had to restrict ourselves towards higher neutron energies. Hence, Fig. 8 contains only data in the neutron energy region between 2 and 5 MeV. Although the statistical accuracy is quite poor, indicated by the large error bars (containing statistical uncertainties and those for background determination as well as for efficiency) and an increased bin size, we fitted a Maxwell-Boltzmann distribution to the data. It results in a temperature parameter $T_{fit} = (1.08 \pm 0.24)$ MeV, which agrees within the error margins with documented values like e.g. $T = 1.29$ MeV [19]. Estimating the average neutron multiplicity $\bar{\nu}$ was not possible, because the problems with the dynode output of the PM tube did not only distort the timing information, but also caused the loss of an unknown amount of events. Admittedly, the data presented here is of poor quality and the shape of the neutron spectrum - a Maxwell-Boltzmann distribution - was known beforehand, still, reasonable agreement with previously published values for the temperature parameter was achieved. This result might at least serve to illustrate the applicability of the neutron detecting technique presented in this work.

4. Summary and outlook

In this paper we have demonstrated how γ-rays produced in inelastic neutron scattering were used to obtain information about the incident neutron spectrum as well as properties of materials like cross sections or spatial distributions. This was possible because of the excellent timing resolution in combination with a good resolving power of $LaBr_3 : Ce$ detectors, which makes it possible to separate neutron-induced events by means of the time-of-flight method. Three applications were presented:

- Known reaction cross section and incident neutron spectrum allow for a "one-dimensional tomography", i.e. the relative abundance of iron was determined and identified as the fission fragment spectrometer VERDI. In

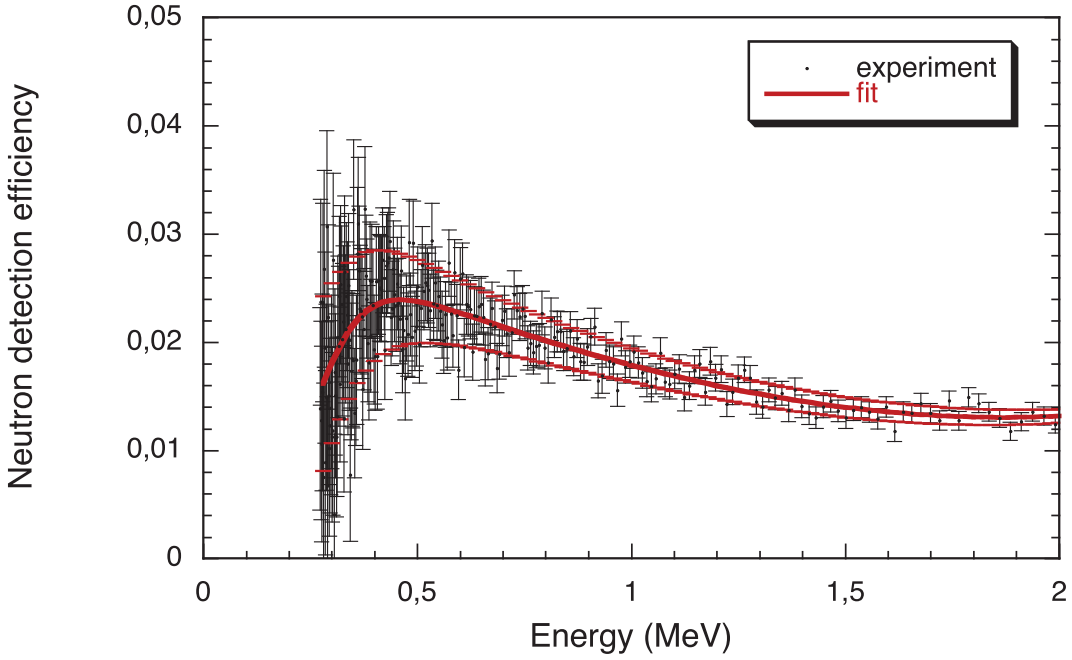

Figure 7: Experimental neutron efficiency as a function of neutron energy together with the result of a fit.

order to obtain more than just radial information about an object, i.e. information about the distance between a certain material and the detector, more detectors at placed at different angles and an appropriate algorithm seems to be necessary.

- Known neutron spectrum and geometry of the scattering object makes it possible to determine reaction cross sections as function of energy, here shown for inelastic neutron scattering off ^{79,81}Br, which is present in the detector. In order not to distort the incident neutron spectrum, this technique should be employed in a low scattering environment.

- If the geometry of the scattering object (here: the $LaBr_3$: Ce detector itself) and the cross section for the reaction of interest (here: inelastic neutron scattering) are known, this information may be used to determine the incident particle spectrum (here: neutrons). Since the detection efficiency is related to the cross section for the reaction, the reaction examined in this work provides a low threshold of about 280 keV, which is much lower than for standard neutron detectors [20]. The observed efficiency between 2 and 3% is quite low, but we believe that this might be improved by using detectors with larger volume and by choosing other reactions and/or materials providing the γ-rays that are to be detected.

Efforts on realizing the above mentioned improvements are on-going and a new experiment to measure both prompt fission γ-rays and fission neutrons from the reaction ^{235}U(n$_{th}$,f) is granted and scheduled for May/June 2012. We hope that the technique of detecting neutrons presented in this work will offer a replacement technology for neutron monitoring, which today involves counters based on ^{3}He, whose shortage is reported to be imminent in the very near future [21].

One of the authors (R. B.) is indebted to the European Commission for providing a PhD fellowship at EC-JRC IRMM, during which part of this work was carried out.

References

[1] R. Billnert, S. Oberstedt, E. Andreotti, M. Hult, G. Marissens, A. Oberstedt, Nucl. Instr. Meth. A 647 (2011) 94.

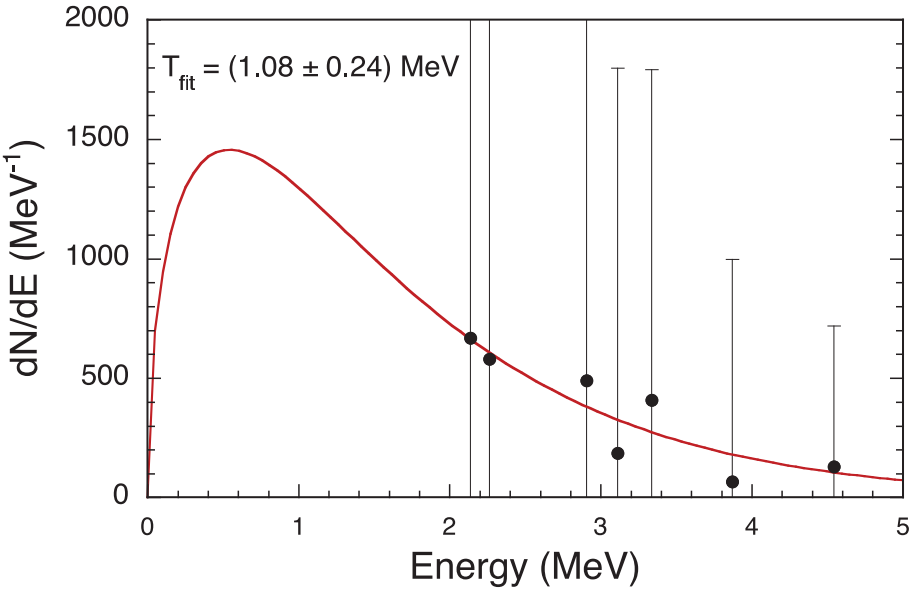

Figure 8: Energy spectrum of neutrons from the reaction ^{235}U(n_{th}, f). The experimental values are fitted to a Maxwell-Boltzmann distribution in order to extract a temperature parameter.

[2] A. Oberstedt, S. Oberstedt, R. Billnert, W. Geerts, F.-J. Hambsch, and J. Karlsson, Nucl. Instr. Meth. A 668 (2012) 14.
[3] Nuclear Data High Priority Request List of the NEA (Req. ID: H.3, H.4), http://www.nea.fr/html/dbdata/hprl/hprlview.pl?ID=421 and http://www.nea.fr/html/dbdata/hprl/hprlview.pl?ID=422.
[4] A. Oberstedt, R. Billnert, J. Karlsson, A. Göök, S. Oberstedt, F.-J. Hambsch, X. Ledoux, J.-G. Marmouget, T. Belgya, Z. Kis, L. Szentmiklosi, K. Takács, T. Martinez-Perez, D. Cano-Ott, Proceedings of Seminar on Fission VII, Het Pand, Gent, Belgium, May 16-20, 2010, eds. C. Wagemans, J. Wagemans and P. Dhondt, World Scientific, ISBN-13 978-981-4322-73-7 (2010) 223.
[5] A. Oberstedt, R. Billnert, A. Göök, J. Karlsson, S. Oberstedt, F.-J. Hambsch, R. Borcea, T. Martinez-Perez, D. Cano-Ott, T. Belgya, Z. Kis, L. Szentmiklosi, and K. Takács, Proceedings of Final Scientific EFNUDAT Workshop, Geneva, Switzerland, August 30 - September 2, 2010, in press.
[6] S. Oberstedt, T. Belgya, R. Billnert, R. Borcea, A. Göök, F.-J. Hambsch, J. Karlsson, Z. Kis, X. Ledoux, J.-G. Marmouget, T. Martinez, A. Oberstedt, L. Szentmiklosi, K. Takács, Proceedings of THEORY-1 Scientific Workshop on Nuclear Fission Dynamics and the Emission of Prompt Neutrons and Gamma Rays, Sinaia, Romania, 27-29 September 2010, in press.
[7] Saint-Gobain Crystals, http://www.detectors.saint-gobain.com/.
[8] A. Oberstedt, R. Billnert, S. Oberstedt, manuscript to be submitted to Nucl. Instr. Meth. A.
[9] BrilLanCe380-data-sheet.pdf, http://www.detectors.saint-gobain.com/.
[10] S. Oberstedt, R. Borcea, Th. Gamboni, W. Geerts, F.-J. Hambsch, R. Jaime Tornin, A. Oberstedt, and M. Vidali, Proceedings of EFNUDAT Slow and Resonance Neutrons, Scientific Workshop on Neutron Data Measurements, Theory and Applications, Budapest, Hungary, September 23 - 25, 2009, ed. T. Belgya, ISBN 978-963-7351-19-8 (2010).
[11] S. Oberstedt, R. Borcea, F.-J. Hambsch, Sh. Zeynalov, A. Oberstedt, A. Göök, T. Belgya, Z. Kis, L. Szentmiklosi, K. Takács, T. Martinez-Perez, Proceedings of Seminar on Fission VII, Het Pand, Gent, Belgium, Ed. C. Wagemenas, J. Wagemans, P. D'hondt, World Scientific, ISBN-13 978-981-4322-73-7 (2010) 207.
[12] I. Fabry and F.-J. Hambsch, GENDARC: The GEel Neutron physics Data acquisition, Analysis and Run Control program, JRC Technical Notes GE/NP/01/2008/01/13 (2008).
[13] RITVERC GmbH, http://www.ritverc.com.
[14] "Physics of Neutron Emission in Fission", INDC(NPS)-220, International Atomic Energy Agency (1989).
[15] N.V. Kornilov, A.B. Kagalenko, S.V. Poupko, P.A. Androsenko, and F.-J. Hambsch, Nucl. Phys. A 686 (2001) 187.
[16] http://www.oecd-nea.org/tools/abstract/detail/nea-1669/
[17] http://www.oecd-nea.org/
[18] K. Shibata, O. Iwamoto, T. Nakagawa, N. Iwamoto, A. Ichihara, S. Kunieda, S. Chiba, K. Furutaka, N. Otuka, T. Ohsawa, T. Murata, H. Matsunobu, A. Zukeran, S. Kamada and J. Katakura, Journal of Nuclear Science and Technology, Vol. 48 (2011) 1, available by JANIS-3.2, OECD Nuclear Energy Agency, http://www.oecd-nea.org/janis/.
[19] K.S. Krane, Introductory Nuclear Physics, John Wiley & Sons, ISBN 0-471-80553-X (1988).
[20] N.V. Kornilov, I. Fabry, S. Oberstedt, F.-J. Hambsch, Nucl. Instr. Meth. A 599 (2009) 226.
[21] R.T. Kouzes, J.H. Ely, L.E. Erikson, W.J. Kernan, A.T. Lintereur, E.R. Siciliano, D.L. Stephens, D.C. Stromswold, R.M. Van Ginhoven, M.L. Woodring, Nucl. Instr. Meth. A 623 (2010) 1035.